



Graphene oxide photocatalyst loaded with Bi₂O₃ for efficient rhodamine B photocatalytic degradation.

Sara Saad Eshak , Shady M. El-dafrawy, Awad I. Ahmed

Chemistry department, Faculty of science, Mansoura University, Egypt)

* Correspondence to: sarasaadeshak@icloud.com, 01003921917

Received: 24/1/2025
Accepted: 29/4/2025

Abstract: A facile method was applied for synthesis of graphene oxide based on bismuth oxide (Bi₂O₃) by hydrothermal method. Thermal treatments were applied to the produced composite (5%β- GO/Bi₂O₃) at 350 °C. Rhodamine-B (RhB) degradation under UV and visible light was investigated to determine the composites' photocatalytic activity. The effects of calcination temperature, dye concentration, and initial pH of dyes were studied on photocatalytic degradation of organic dye. The prepared composites showed good enhancement on photocatalytic degradation compared with pure Bi₂O₃. This high performance of composites is attributed to the good distribution of Bi₂O₃ particles on the graphene oxide sheets, rapid transfer of the photogenerated electron on the surface that led to decrease the hole electron recombination.

Keywords: Bismuth Oxide (Bi₂O₃), Graphene Oxide (GO), Photocatalytic degradation, rhodamine-B (Rh B).

1. Introduction

Environmental contamination, particularly water pollution, has increased in recent years due to modern industry's rapid growth. Since the water environment is one of the sources of life for living things, pollution of the water environment is a serious issue that needs to be resolved.

Industrial and medical waste can contribute significantly to water pollution issues if it is dumped into a river without any additional treatment. The rhodamine B (RhB) dye, which is widely used in the food, leather, and textile sectors[1] , causes a number of ecological issues because it inhibits light penetration in water, which lowers photosynthesis in aquatic plants[2] [3]. Additionally, it has been shown that this dye is mutagenic and carcinogenic. Therefore, rhodamine B can build up in the digestive tracts of humans and animals through nutrition, leading to a number of digestive disorders, including liver failure, intestinal tumours, and stomach polyps [4]. According to research, the dye is extremely neurotoxic and carcinogenic to living things . The waste's toxic, buildup-prone, and potentially cancer-causing nature poses a significant danger to the aquatic environment.

Therefore, to address this issue of water contamination, an effective and efficient approach is required. Advanced Oxidation Processes (AOPs) are a popular green procedure that is economical and ecologically benign, making them more efficient in solving water-related environmental issues. In AOPs, hydroxyl radicals are produced in large enough amounts to influence water purification and make use of the oxidation reaction process. [5] [6] Because photocatalytic technology can perform oxidation reactions, produce hydroxyl radicals, and is environmentally benign and sustainable, it has good potential for usage in this technique.[7, 8] Semiconductor photocatalysts have been used extensively to address the issue of water contamination. Titanium Oxide TiO₂ with other semiconductors Bi₂O₃, SnO₂, and ZnO have been largely applied to degrade pollutants in the aquatic environment under Ultraviolet (UV) light irradiation.[9]

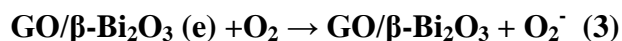
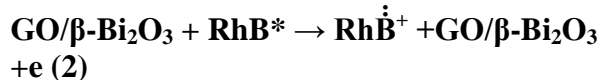
As well as established methods, chemical stability of semiconductors against photo corrosion, catalysis has played an important role in the degradation of organic pollutants, The foundation of heterogeneous photocatalysis is the creation of electron-hole pairs

by stimulating a semiconductor with radiation, usually in the ultraviolet. To create radicals like $O_2^{\cdot -}$ and OH^{\cdot} , these species react with molecules that have been absorbed on the surface, including contaminants, oxygen, water, and hydroxyl ions. Traditional oxidants may mineralize most organic molecules either completely or partially, but these radicals have a greater oxidizing potential. [10-12]

Bi_2O_3 is proving to be one of the most important and suitable photocatalysis for application in the environment due to its biological nontoxicity[6, 10, 13, 14], ability to redox, and lower cost. But its relatively wide band gap (3.2 eV) and high rate of photogenerated electron/hole recombination limit its further application in visible light vision ($400\text{ nm} < \lambda < 700\text{ nm}$) with hydrothermal method by using graphene oxide as a dispersant[15-17], which might improve the distribution of particles during ultrasonication. Photodegradation of rhodamine-B (RhB) was employed to investigate the photocatalytic activities of the Bi_2O_3 /GO photocatalyst, with 500 w Xe-lamp equipped with a U.V - cut-off filter ($\lambda > 400\text{ nm}$) as the light source. To support Bi_2O_3 semiconductors, GO was selected.[18, 19] This structure has never been recorded as far as we know. In comparison to semiconductors Bi_2O_3 alone, our ternary GO/Bi_2O_3 combination, which was made using the Hydro-thermal process and calcined at various temperatures, has demonstrated its efficacy in photodegradation of RhB, particularly when calcined at 350°C .

The degradation reaction process was monitored by measuring the concentration of RhB as a function of irradiation time in the solution with UV-Vis absorption spectrum. All the photocatalytic experiments in this article were carried out at neutral pH. Through high photon energy irradiation, electrons move from the VB to the CB in the photocatalyst. By creating holes and electrons on the valence and conduction bands, respectively, electron-hole pairs are induced. The hole oxidizes water molecules to produce hydrogen gas and hydroxyl radicals, while the electrons transform oxygen atoms into superoxide radicals. After that, the superoxide and hydroxyl radicals attack the pollutants and turn them into

harmless byproducts. The following equations illustrate the mechanism of the photocatalytic activity process.[12, 20]



2. Materials and procedures

2.1. Materials and chemicals

All of the chemicals utilized came from commercial sources without any additional purification. Alpha Aesar provided 99.9 % graphite powder, while ADWIC provided 30 % hydrogen peroxide (H_2O_2), concentrated sulfuric acid (H_2SO_4), potassium permanganate ($KMnO_4$), and sodium nitrate ($NaNO_3$). Sigma Aldrich supplied ammonium hydroxide (NH_4OH), bismuth (III) nitrate ($Bi(NO_3)_3 \cdot 5H_2O$), absolute ethanol, and rhodamine B (RhB).

2.2. Synthesis of Graphene Oxide (GO)

GO was produced utilizing powdered flake graphite and the improved Hummers technique. After 1 g of $NaNO_3$ has completely dissolved in 12.5 mL of concentrated H_2SO_4 , 1.0 g of graphite powder (99.95%) is added. The mixture must be aggressively agitated in an ice bath and kept at 0°C for two hours. After the addition of 2.0 g of $KMnO_4$ gradually over the period of 1.5 hours and then the mixture was cooled for 2 hours in an ice bath. After that, the mixture was vigorously stirred and let to remain at room temperature for twenty-four hours. 50 mL of deionized H_2O was added slowly to the paste, causing violent effervescence and the evolution of brown vapour. After 15 minutes, 100 mL of deionized H_2O was added to the mixture. 15 mL of H_2O_2 (30%) was added to reduce the residual $KMnO_4$, and the suspension turned golden yellow with bubbling. The solution was then washed three times with HCl (10%) and then with H_2O until the residual H_2SO_4 was completely removed, as determined by $BaCl_2$. Finally, the mixture was dried at 80°C overnight to obtain GO sheets.

2.3. Synthesis of 5% $\beta-Bi_2O_3$ /GO

The Bi_2O_3 /GO was made utilizing a hydrothermal process with mild conditions and

a precursor of $\text{Bi}(\text{NO}_3)_3 \cdot 5\text{H}_2\text{O}$. The reaction begins with the dissolution of 1.0 g of bismuth nitrate pentahydrate $\text{Bi}(\text{NO}_3)_3 \cdot 5\text{H}_2\text{O}$ in 10 mL of diluted HNO_3 solution (0.75 M). In a typical case, $\text{Bi}(\text{NO}_3)_3 \cdot 5\text{H}_2\text{O}$ was dissolved in nitric acid to avoid hydrolyzation of Bi^{3+} ions containing an equivalent amount of GO. Ammonia solution NH_4OH was added after full dissolution while being vigorously stirred for three to four hours to maintain the precipitation reaction's pH value at 8.5. After being moved to a 100 mL Teflon-lined stainless-steel autoclave, the resulting was heated and kept at 180°C . Finally, the product was centrifuged, washed several times, dried at 80°C , and calcined at 350°C .

2.4. Material Characterization

The effectiveness of the preparation was verified using a range of analytical methods. Using an SEM (JEOL JSM 6510lv), the morphology (microstructure) of the tailored composite was examined. The crystal structure at the 2θ range of $5\text{--}70^\circ$ was analyzed using Bruker equipment ($\lambda = 1.54178 \text{ \AA}$, step size of 0.02 and scan step length of 0.80 s) and X-ray diffraction (XRD) patterns.

3. Results and Discussion

3.1. Specifications of the Material

Fig.1 shows the TEM image of the precursor of the 5%GO/ $\beta\text{-Bi}_2\text{O}_3$ sample, while its particles exhibit an approximate diameter of 2.3-7.2 nm. It can be found in Fig.1 that the tetrahedral structures of the Bi_2O_3 sample are constructed by GO accumulating nanosheet layer by layer. On the other hand, the GO/ $\beta\text{-Bi}_2\text{O}_3$ functional groups were identified via FT-IR analysis (Fig. 2). The skeletal vibrations of graphitic domains are responsible for the $\text{C} = \text{C}$ peak at 1631 cm^{-1} and the broad and strong O-H peak at 3438 cm^{-1} that results from intercalated water [11, 24]. Carboxylic acid and carbonyl groups' stretching vibration modes of $\text{C} = \text{O}$ are responsible for the strong band at 1631 cm^{-1} , while C-O (epoxy) groups are responsible for the band at 1249 cm^{-1} .

Fig.3 shows the x-ray pattern of the as-prepared sample of Bi_2O_3 shows peaks at 2θ values of $27.5, 30.16, 39.07, 46.95,$ and 51.67° , which correspond to (2 0 1), (2 1 1), (2 2 0), (4 0 0), and (2 0 3) respectively, crystal planes. It proves the forming of the pure Bi_2O_3 (β -

phase). The intense peaks indicate that tetragonal $\beta\text{-Bi}_2\text{O}_3$ owns a good crystallization.

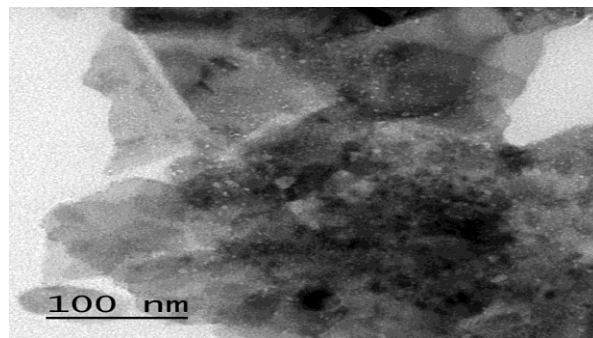


Fig. 1: TEM images of 5% $\text{Bi}_2\text{O}_3/\text{GO}$.

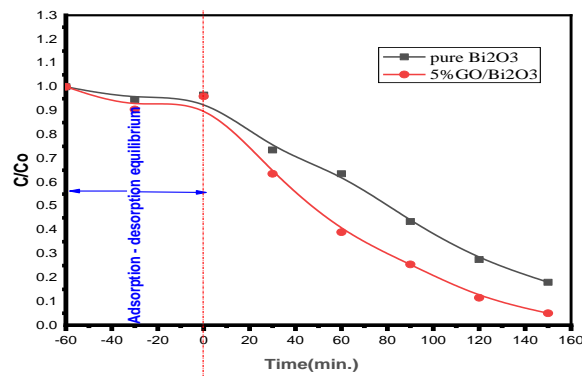


Fig. 2: FT-IR image of 5% $\text{Bi}_2\text{O}_3/\text{GO}$.

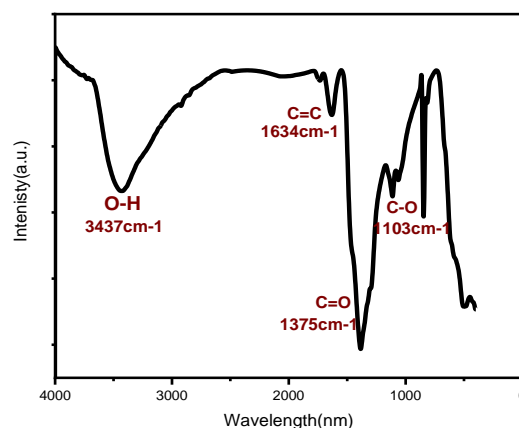


Fig. 3: X-ray image of 5% $\text{Bi}_2\text{O}_3/\text{GO}$.

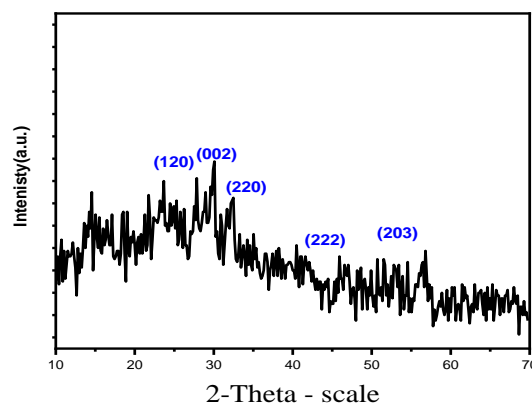


Fig. 4: Removal of RhB dye using pure Bi_2O_3 and 5% $\text{Bi}_2\text{O}_3/\text{GO}$ calcined at 350°C

3.2. Photocatalytic performance of calcined $\text{Bi}_2\text{O}_3/\text{GO}$

In comparison to the photocatalysts, the parent before loading of GO exhibits poorer performance for the photo-degradation of RhB (only 62% within 2.5 hours). Compared to pure $\beta\text{-Bi}_2\text{O}_3$, the 5% GO/ $\beta\text{-Bi}_2\text{O}_3$ sample calcinated at 350 °C shows the best performance where the degradation efficiency of RhB reaches 96.5% after 2.5 h. Further increase of the calcination temperatures exerts a negative effect on the degradation performances, as observed in Fig.4.

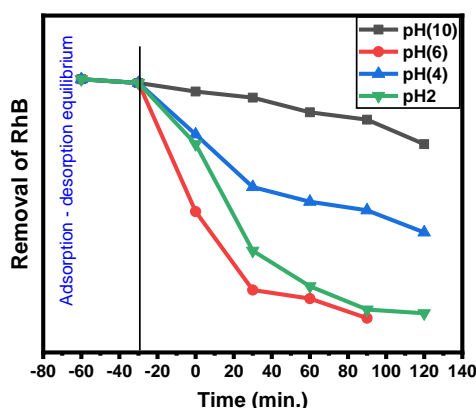


Fig. 5: Removal of RhB dye using 5% $\text{Bi}_2\text{O}_3/\text{GO}$ at different pH.

Fig. 5 shows the effectiveness of pH on RhB degradation using 5% $\beta\text{-Bi}_2\text{O}_3/\text{GO}$ photocatalyst calcined at 350 °C. It is known that the pH of solution may influence the photocatalytic activity. So, the effect of pH was studied by adjusting pH of the solutions with NaOH and HCl. The Rhodamine-B degradation experiments were performed in the pH range of 2.0-10.0 with a photocatalyst dosage of 0.05 g/L. The initial pH value of the Rh-B solution in natural conditions was 6. The degradation ability of GO/ $\beta\text{-Bi}_2\text{O}_3$ for Rd-B decreased after adjusting the pH of solutions. As shown in Fig. 5, the highest photocatalytic activity was observed at the pH value of 6.0.

4. Conclusion

A series of $\text{Bi}_2\text{O}_3/\text{GO}$ composite were prepared in this study using the nonaqueous hydrothermal technique, and they showed improved photocatalytic activity and stability in the destruction of Rh-B when exposed to visible light. Compared to pure GO, the addition of Bi_2O_3 may significantly inhibit the

overgrowth of crystallites and improve absorption of visible light. In addition the effect of pH of solutions was studied and the results confirmed that the high photocatalytic activity was obtained at pH value of 6.

References

1. L. Zhang, Y. Meng, H. Shen, J. Li, C. Yang, B. Xie, S. Xia, (2021) Photocatalytic degradation of rhodamine B by $\text{Bi}_2\text{O}_3/\text{LDHs}$ S-scheme heterojunction: Performance, kinetics and mechanism, *Appl Surf Sci*, **567** 150760.
2. X. Chen, J. Dai, G. Shi, L. Li, G. Wang, H. Yang, (2016) Sonocatalytic degradation of Rhodamine B catalyzed by $\beta\text{-Bi}_2\text{O}_3$ particles under ultrasonic irradiation, *Ultrason Sonochem*, **29** 172-177.
3. A.M. Al-Hamdi, U. Rinner, M. Sillanpää, (2017) Tin dioxide as a photocatalyst for water treatment: A review, *Process Safety and Environmental Protection*, **107** 190-205.
4. M. Ali, P. Swami, A. Kumar, D. Guin, C.S.P. Tripathi, (2024) Enhanced photocatalytic degradation of Rhodamine B using gold nanoparticles decorated on BaTiO_3 with surface plasmon resonance enhancement, *Anal Sci*, **40** 643-654.
5. Z. Miao, Y. Tian, S. Li, Z. Ding, X. Chen, W. Ma, Y. Chang, (2022) Photocatalytic degradation of Rhodamine B over popcorn-like $\text{ZnFe}_2\text{O}_4/\text{CdS}-\text{GO}$ ternary composite, *Journal of Materials Research and Technology*, **21** 1863-1877.
6. D. Xu, Y. Hai, X. Zhang, S. Zhang, R. He, (2017) Bi_2O_3 cocatalyst improving photocatalytic hydrogen evolution performance of TiO_2 , *Appl Surf Sci*, **400** 530-536.
iopscience.iop.org/article/10.1088/1757-899X/107/1/012006/pdf.
7. L. Liu, M. Xu, Y. Ye, B. Zhang, (2022) On the degradation of (micro)plastics: Degradation methods, influencing factors, environmental impacts, *Sci Total Environ*, **806** 151312.
8. P. Shandilya, A. Sudhaik, P. Raizada, A. Hosseini-Bandegharai, P. Singh, A. Rahmani-Sani, V. Thakur, A.K. Saini, (2020) Synthesis of Eu^{3+} -doped $\text{ZnO}/\text{Bi}_2\text{O}_3$ heterojunction photocatalyst

- on graphene oxide sheets for visible light-assisted degradation of 2,4-dimethyl phenol and bacteria killing, *Solid State Sciences*, **102** 106164.
9. P. Qiu, B. Park, J. Choi, M. Cui, J. Kim, J. Khim, (2017) BiVO₄/Bi₂O₃ heterojunction deposited on graphene for an enhanced visible-light photocatalytic activity, *J Alloys Compd*, **706** 7-15.
 10. M. Usman, M. Humayun, S.S. Shah, H. Ullah, A.A. Tahir, A. Khan, H. Ullah, (2021) Bismuth-Graphene Nanohybrids: Synthesis, Reaction Mechanisms, and Photocatalytic Applications—A Review, *Energies*, **14** 2281.
 11. J. Angelo, L. Andrade, L.M. Madeira, A. Mendes, (2013) An overview of photocatalysis phenomena applied to NO_x abatement, *J Environ Manage*, **129** 522-539.
 12. Y. Shi, L. Luo, Y. Zhang, Y. Chen, S. Wang, L. Li, Y. Long, F. Jiang, (2017) Synthesis and characterization of α/β -Bi₂O₃ with enhanced photocatalytic activity for 17 α -ethynylestradiol, *Ceramics International*, **43** 7627-7635.
 13. K.M.C.A.I. (2021) Department of Chemistry, F.S. Ali, M. Ragamathunnisa, G.A.C.f.W.P.I. Department of Physics, F. Al Marzouqi, C.o.S.S.Q.U.M.O. Department of Chemistry, A.R.M. Jahangir, M.A.F.P.C.M.S.o.O. Biyaq Oilfield Services Llc Post Box, A. Ayeshamariam, K.M.C.A.I. Department of Physics, K. Kaviyarasu, U.-U.A.C.i.N.N.L.C.o.G.S.U.o.S.A.M.R.P.O. B.P.S.A. Kasinathan Kaviyarasu, M.R.G.i.L.-N.R.F.O.F.R.P.O.B.S.W.W.C.P.S.A. Nanosciences African network, Synthesis and characterization of Bi₂O₃ NPS and photocatalytic application with methylene blue, *J. Optoelectron. Biomed. M.*, **13** 95-106.
 14. N. Wang, J. Xu, L. Guan, (2011) Synthesis and enhanced photocatalytic activity of tin oxide nanoparticles coated on multi-walled carbon nanotube, *Mater Res Bull*, **46** 1372-1376.
 15. V. Mane, D. Dake, N. Raskar, R. Sonpir, E. Stathatos, B. Dole, (2024) A review on Bi₂O₃ nanomaterial for photocatalytic and antibacterial applications, *Chemical Physics Impact*, **8** 100517.
 16. Q. Xu, L. Zhang, B. Cheng, J. Fan, J. Yu, S-Scheme (2020) Heterojunction Photocatalyst, *Chem*, **6** 1543-1559.
 17. W.S. Hummers, R.E. Offeman, (1958) Preparation of Graphitic Oxide, *J Am Chem Soc*, **80** 1339-1339.
 18. H.S. Park, H.-W. Ha, R.S. Ruoff, A.J. Bard, (2014) On the improvement of photoelectrochemical performance and finite element analysis of reduced graphene oxide-BiVO₄ composite electrodes, *Journal of Electroanalytical Chemistry*, **716** 8-15.
 19. F. Mohamadpour, A.M. Amani, (2024) Photocatalytic systems: reactions, mechanism, and applications, *RSC Adv*, **14** 20609-20645.